

Supramolecular Structural Diversity among First-Generation Hybrid Dendrimers and Twin Dendrons

Virgil Percec,*^[a] Jonathan G. Rudick,^[a] Mihai Peterca,^[a, b] Michael E. Yurchenko,^[a] Jan Smidrkal,^[a] and Paul A. Heiney^[b]

Abstract: Hybrid dendrimers, obtained by complete monofunctionalization of the peripheral amines of a “zero-generation” polyethyleneimine dendrimer, provide structurally diverse lamellar, columnar, and cubic self-organized lattices that are less readily available from other modified dendritic structures. The reaction of tris(2-aminoethyl)amine (TREN) with 4-dodecyloxylbenzimidazolide provides only the corresponding zero-generation TREN dendrimer. From the mixture of tri- and disubstituted TREN derivatives obtained from first-generation self-assembling dendritic imidazolides, the

hybrid dendrimer and a twin dendron could be separated, purified, and characterized. The hybrid dendrimers display smectic, columnar hexagonal (Φ_h), and cubic ($Pm\bar{3}n$) lattices. The TREN twin dendrons, on which only two peripheral amines have been acylated, exhibit centered-rectangular columnar (Φ_{rc}), Φ_h , and $Pm\bar{3}n$ lattices. The existence of a thermoreversible Φ_h -to- $Pm\bar{3}n$ phase transition in the first-genera-

Keywords: dendrimers • liquid crystals • self-assembly • supramolecular chemistry

eration hybrid dendrimers and twin dendrons is exploited to elucidate an epitaxial relationship between the two mesophases. We postulate a mechanism by which the transition proceeds. The thermoreversible Φ_h -to- $Pm\bar{3}n$ phase change is accompanied by optical property changes that are suitable for rudimentary signaling or logic functions. This structural diversity reflects the quasiequivalence of flat-taper and conical self-assembling dendrons and the ability of flexible dendrimers to accommodate concomitant conformational and shape changes.

Introduction

Self-assembling dendrons and dendrimers available through divergent^[1] and convergent^[2] synthetic strategies are powerful monodisperse architectures with which to investigate how primary structure manifests in the formation of three-dimensional (3D) superstructures.^[3] Dendrons and dendrimers that form liquid crystalline phases,^[3c,4] in particular, have shown tremendous potential for the control of molecular and supramolecular properties. The emergent mesophases

and novel functions that arise through hierarchical self-assembly and self-organization are the basis for the elaboration of new concepts relevant for macromolecular and supramolecular chemistry, as well as the nanosciences. Furthermore, structural and retrostructural analysis of the self-organized arrays facilitates elucidation of the design principles that underlie the hierarchical self-assembly process.^[3c]

Several architectural classes can be identified among dendrons and dendrimers that form liquid-crystalline mesophases.^[4] We have pioneered the use of mesogenic repeat units to prepare dendrons and dendrimers^[5] and the use of amphiphilic self-assembling dendrons to generate supramolecular dendrimers^[6] and self-organizable dendronized polymers.^[7] An alternative approach is to append mesogens to the periphery of nonmesogenic dendrimers.^[8] We have further extended this approach to the functionalization of Fréchet-type^[2a] AB_4 ,^[9] and AB_5 ^[9] dendrons with amphiphilic self-assembling dendrons.^[9,10] Nonmesogenic dendrons and dendrimers appended with peripheral mesogens display limited structural diversity,^[4,8,10] especially when contrasted with the rich structural complexity available from the supramolecular dendrimers^[6] and self-organizable dendronized polymers^[7].

[a] Prof. Dr. V. Percec, Dr. J. G. Rudick, Dr. M. Peterca, Dr. M. E. Yurchenko, J. Smidrkal Roy & Diana Vagelos Laboratories Department of Chemistry University of Pennsylvania Philadelphia, PA 19104-6323 (USA) Fax: (+1)215-573-7888 E-mail: percec@sas.upenn.edu

[b] Dr. M. Peterca, Prof. Dr. P. A. Heiney Department of Physics and Astronomy University of Pennsylvania Philadelphia, PA 19104-6396 (USA)

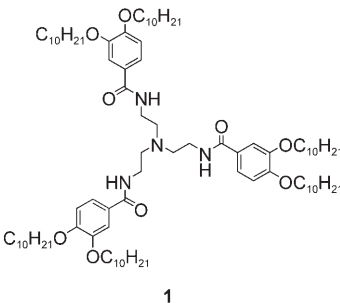
derived from amphiphilic self-assembling dendrons. Lamellar, various two-dimensional (2D) columnar, and 3D cubic, tetragonal, and 12-fold liquid-quasicrystal arrays have been identified.^[6,7]

Hybrid dendrons and dendrimers combine two constitutively different building blocks. This expands our previous definition of “hybrid” dendrons as those composed of non-dendritic ((AB)_y) and dendritic (AB_n) building blocks.^[11] As such, this term now includes dendrons composed of combinations of (AB₂) with (AB₃) building blocks^[6a-d,10] and of (AB₂) or (AB₃) with (AB₄) or (AB₅) building blocks.^[9] Examples of branched compounds that are not amenable to elaboration with dendrimers have been appended with self-assembling dendrons and exhibit liquid-crystalline phases.^[12] These too constitute hybrid dendrimers. Self-assembling hybrid dendrons and dendrimers are distinct from dendritic molecules functionalized at their periphery with traditional mesogens.^[4]

Herein, we present a strategy by which to increase the supramolecular structural diversity available with dendrimers by using hybrid dendrimers. Hybrid dendrimers are composed of two or more constituent elements, each of which is capable of elaborating a perfectly branched molecular structure independent of the other. The present hybrid dendrimers are obtained by acylation of the prototypical “zero-generation” polyethyleneimine (PEI) dendrimer, tris(2-aminoethyl)amine (TREN), with 4-dodecyloxybenzimidazolide,^[13] or first-generation self-assembling dendritic imidazolides.^[13] Either trisubstituted dendrimers or disubstituted twin dendrons^[14] are obtained. The hybrid dendrimers display smectic, columnar hexagonal (Φ_h), and cubic ($Pm\bar{3}n$) lattices. Similarly, the twin dendrons exhibit centered-rectangular (Φ_{r-c}), Φ_h , and $Pm\bar{3}n$ lattices. Furthermore, we observe thermoreversible phase changes accompanied by changes in optical properties that are suitable for rudimentary signaling or logic functions. A Φ_h -to- $Pm\bar{3}n$ phase transition reported herein reveals an epitaxial relationship between the Φ_h and $Pm\bar{3}n$ lattices. Based on this relationship, we have postulated a mechanism by which the transition between the two mesophases can occur. This mechanism may be relevant to other supramolecular dendrimers,^[10b] dendronized polymers,^[15d-g] and metallocmesogens^[16] exhibiting a similar columnar-to-cubic phase transition.

Results and Discussion

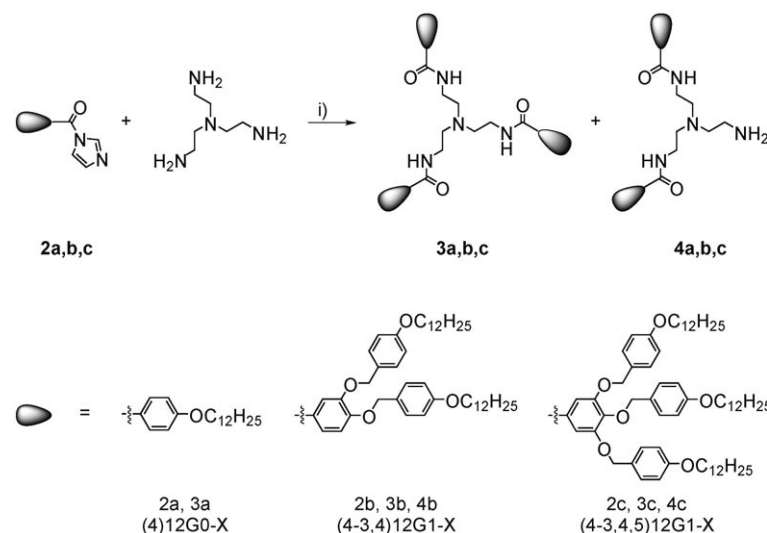
Zero- and first-generation PEI dendrimers have previously been functionalized with 3,4-bis(decyloxy)benzoate groups (for example, **1**)^[8b,c] as architec-



tural congeners to liquid-crystalline cyclic oligomers^[17] and linear polymers.^[15] The dendrimers were prepared by the reaction of the PEI dendrimer with the dendritic benzoyl chloride.^[8b,c] While the first-generation dendrimer does not display any mesophases,^[8b] the second-generation dendrimer was found to form a Φ_h phase.^[8c] Both first- and second-generation dendrimers exhibit mesophases upon complexation of transition-metal salts.^[8c] A lamellar phase is most common among the transition-metal complexes of **1**.

We have employed larger first-generation self-assembling dendrons, which are acid sensitive, to explore supramolecular structural diversity within low-generation hybrid dendrimers. Consequently, we sought a synthetic strategy that would avoid the benzoyl chloride intermediate. Imidazolides **2a-c** (Scheme 1) have recently been prepared through reaction of 1,1-carbodiimidazole (CDI)^[18] with the corresponding dendritic carboxylic acid.^[13] The imidazolides can be isolated and stored in the absence of moisture. Reaction of the imidazolide with TREN provided a mixture of di- and triacylated products (Scheme 1). The structures and purities of dendrimers **3a-3c** and the twin-dendritic compounds **4b** and **4c** were confirmed by a combination of ¹H and ¹³C NMR spectroscopy, HPLC, and MALDI-TOF mass spectrometry.

Differential scanning calorimetry (DSC) and thermal optical polarized microscopy (TOPM) were used to identify



Scheme 1. Synthesis of hybrid dendrimers and twin dendrons. a) THF.

phase transitions and establish preliminary phase assignments. The phase assignments were confirmed by X-ray diffraction (XRD) (Figure 1). Table 1 presents phase-transition temperatures and corresponding enthalpy changes for each of the hybrid dendrimers and twin dendrons. The zero-generation hybrid dendrimer **3a** exhibits a narrow smectic phase, which is consistent with the previous observation for transition-metal salts of **1**.^[8] The first-generation hybrid den-

dimers and twin dendrons exhibit columnar or cubic mesophases, or both.

Table 2 provides the structural and retrostructural analysis of the self-organized lattices generated by the hybrid dendrimers and twin dendrons. Both first-generation hybrid dendrimers self-assemble into supramolecular spheres that self-organize into a $Pm\bar{3}n$ lattice. We have previously shown^[6a,e,f] that this lattice is composed of micellar spherical supramolecular dendrimers resulting from the self-assembly and self-organization of the hybrid dendrimers and twin dendrons. Furthermore, we can contrast this mesophase with the gyroid mesophase formed by other self-assembling dendrons.^[19] The appearance of the $Pm\bar{3}n$ lattice is remarkable given that the constituent dendrons typically form Φ_h phases.^[10] Nonetheless, retrostructural analysis of **3b** and **3c** in the $Pm\bar{3}n$ lattice confirms relationships observed for the constituent dendrons in the Φ_h lattice. The former dendron generates larger supramolecular objects and each supramolecular object is comprised of more molecules. These are seen by comparing the sphere diameters (D) and number of dendrimers per supramolecular sphere (μ ; Table 2). We have previously explained this based on the projected molecular solid angle (a'), whereby the (4-3,4)12G1-X self-assembling dendrons occupy a smaller projected solid angle than the (4-3,4,5)12G1-X self-assembling dendrons (see Scheme 1 for structures). The relationship between the dendron primary structure and features of the tertiary structure are also found for the twin dendrons in the Φ_h phase (Table 2).

Quasiequivalence^[7a,c] of flat-taper and conical self-assembling dendrons results from their conformational flexibility and allows them to behave interchangeably. Self-organizable dendronized polymers take advantage of this by adopting different shapes depending on their degree of polymerization.^[7a,c] We infrequently observe quasiequivalence^[7a,c] that results in reversible shape changes. The first-generation liquid-crystalline PEI dendrimers and twin-dendritic compounds provide two new examples in this small library. We can surmise that the flexible PEI core assists in accommodating the conformational changes that accompany the change in shape.

Models based on the experimental structural and retrostructural analysis of **3c** and **4c** are shown in Figure 2. The models reflect conformations consistent with those expected in the Φ_h lattice. Close inspection of the models reveals that we have intentionally included fewer molecules per column stratum than the number reported for μ in Table 2. The calculation of μ in Table 2 refers to a 4.7 Å-thick column stratum, which is based on the peripheral alkyl chain packing.

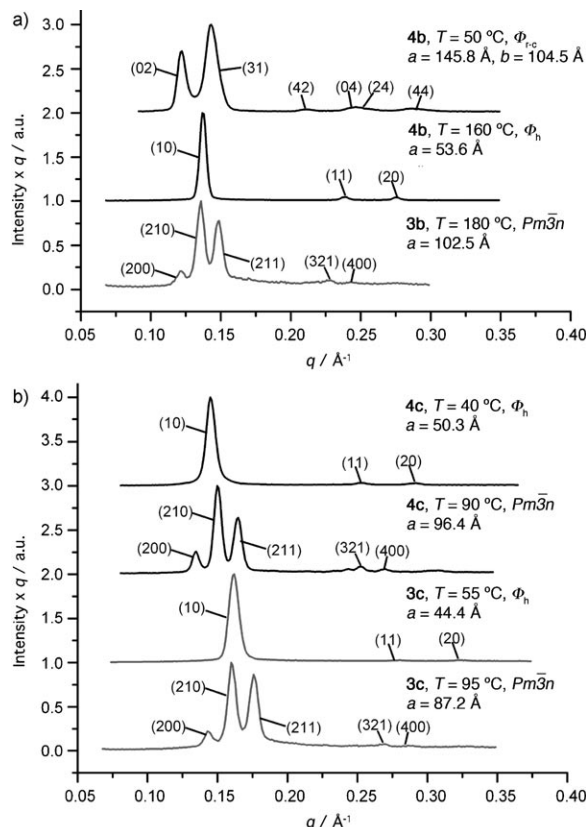


Figure 1. Small-angle XRD powder plots for a) **3b** and **4b** and b) **3c** and **4c**. The structure, temperature, diffraction-peak indexing, and lattice parameters are indicated.

Table 1. Thermal transitions [°C] and corresponding enthalpy changes [kcal mol^{-1}] for the hybrid dendrimers and twin dendrons.^[a]

Compound	First and second heating scans	First cooling scans
3a	$k^{[b]}$ 104 (0.8) $S^{[c]}$ 106 (1.0) $i^{[d]}$ k 101 (0.6) S 104 (6.8) i	i 51 (0.6) S 45 (1.5) k
3b	k 82 (4.8) $x^{[e]}$ 103 (3.2) x 131 (-3.7) x 152 (9.4) $Cub^{[f]}$ 212 (0.6) i Cub 211 (0.5) i	i 208 (0.4) Cub
3c	$\Phi_{h,g}^{[g]}$ 55 $\Phi_h^{[h]}$ 78 (0.7) Cub Φ_h 78 (0.8) Cub	Cub 58 (0.9) Φ_h
4b	k 86 (1.0) x 102 (3.3) x 123 (2.0) x 156 (0.7) Φ_h $\Phi_{rc}^{[i]}$ 67 (-3.9) k 103 (2.5) Φ_{rc} 156 (0.7) Φ_h	Φ_h 153 (0.7) $\Phi_{rc}^{[j]}$
4c	Φ_h 56 (17.9) Cub 160 $dec^{[k]}$	

[a] Thermal transitions [°C] and enthalpy changes [kcal mol^{-1}] in parentheses were determined by DSC (rate: $10^\circ\text{C min}^{-1}$). Data from first heating and cooling scans are on the first line, and data from the second heating scans are on the second line. [b] k : crystalline phase. [c] S : smectic phase. [d] i : isotropic liquid phase. [e] x : unidentified phase. [f] Cub : $Pm\bar{3}n$ cubic lattice. [g] $\Phi_{h,g}$: glassy $p6mm$ hexagonal columnar lattice. [h] Φ_h : $p6mm$ hexagonal columnar lattice. [i] Φ_{rc} : $c2mm$ centered-rectangular columnar lattice. [j] dec : sample decomposes.

Table 2. Structural and retrostructural analysis of the hybrid dendrimers and twin dendrons.

Compound	T [°C]	Phase	$a^{[a,b,c]}$ or $a, b^{[d]}$ [Å]	$d_{10}, d_{20}^{[a]}$ or $d_{110}, d_{200}, d_{210}, d_{211}, d_{220}, d_{310}, d_{321}, d_{400}^{[b]}$ or $d_{10}, d_{11}, d_{20}^{[c]}$ or $d_{20}, d_{11}, d_{02}, d_{22}, d_{13}, d_{40}, d_{31}, d_{42}, d_{24}^{[d]}$ [Å]	D [Å]	μ
3a	50	<i>S</i>	36.5 ^[a]	36.5, 18.3 ^[a]	—	—
3b	180	<i>Pm</i> $\bar{3}$ <i>n</i>	102.5 ^[b]	72.6, 51.4, 45.0, 41.9, 36.3, 32.4, 27.4, 25.6 ^[b]	63.6 ^[e]	36.8 ^[f]
3c	55	Φ_h	44.4 ^[c]	38.5, 22.2, 19.2 ^[e]	44.4 ^[g]	1.6 ^[h]
	95	<i>Pm</i> $\bar{3}$ <i>n</i>	87.2 ^[b]	61.5, 43.6, 39.1, 35.5, 30.8, 27.5, 23.3, 21.7 ^[b]	54.1 ^[e]	16.2 ^[f]
4b	160	Φ_h	53.6 ^[c]	46.4, 26.8, 23.2 ^[c]	53.6 ^[g]	4.6 ^[h]
	50	Φ_{rc}	145.8, 104.5 ^[d]	—, —, 52.4, 42.6, —, —, 44.3, 29.9, 24.6 ^[d]	92.8, ^[i] 104.5 ^[j]	14.4 ^[k]
4c	40	Φ_h	50.3 ^[c]	43.6, 25.2, 21.8 ^[c]	50.3 ^[g]	3.0 ^[h]
	70	<i>Pm</i> $\bar{3}$ <i>n</i>	94.6 ^[b]	67.1, 47.3, 42.5, 38.6, 33.5, 29.9, 25.3, 23.7 ^[b]	58.7 ^[e]	30.4 ^[f]

[a] Layer spacing ($a=0.5[d_{10}+2d_{20}]$) and d spacings of the smectic phase. [b] Lattice parameter ($a=[2^{0.5}d_{110}+2d_{200}+5^{0.5}d_{210}+6^{0.5}d_{211}+8^{0.5}d_{220}+10^{0.5}d_{310}+14^{0.5}d_{321}+16^{0.5}d_{400}]/8$) and d spacings for the *Pm* $\bar{3}$ *n* cubic lattices. [c] Lattice parameter ($a=2/3[d_{10}+3^{0.5}d_{11}+2d_{20}]^{3^{-0.5}}$) and d spacings in the ratio $d_{10}:d_{11}:d_{20}=1:3^{0.5}:2$ for the *p*6*m* lattice of the Φ_h phase. [d] Lattice parameters (a and b) and d spacings for the *c*2*mm* lattice of the Φ_{rc} phase. In general, $a=d_{10}$ and $b=d_{01}$. The ratio of the d spacings can be calculated from the general equation $d_{hk}=((ha^{-1})^2+(kb^{-1})^2)^{-0.5}$. [e] Experimental sphere diameter ($D=8[3a/32\pi]^{0.5}$) in the *Pm* $\bar{3}$ *n* lattices. [f] Number of dendrimers or twin-dendritic molecules per sphere ($\mu=a^3N_A\rho/8M$, where N_A is Avogadro's number (6.0220455×10^{23}), ρ is the density of the polymer (assumed to be 1 g cm^{-3}), and M is the molecular weight of the compound). [g] Experimental column diameter ($D=a$) in the *p*6*m* lattices. [h] Number of dendrimers or twin-dendritic molecules per 4.7-Å-thick column stratum ($\mu=3^{-0.5}aN_Atp/2M$, where t is the column-stratum thickness). [i] Experimental column diameter along the a direction of the *c*2*mm* lattice ($D=a$). [j] Experimental column diameter along the b direction of the *c*2*mm* lattice ($D=b$). [k] Number of dendrimers or twin-dendritic molecules per elliptical 4.7-Å-thick column stratum in the *c*2*mm* lattice of the Φ_{rc} phase ($\mu=abN_Atp/2M$).

Packing of the interior benzyl ether segments is typically much closer, so the models reflect a 3.5 Å-thick column stra-

tum. Recalculation of μ bears out the number of dendrons shown in Figure 2.

Closer packing at the core of the hybrid-dendrimer and twin-dendron supramolecular columns facilitates hydrogen bonds along the length of the column. A network of possible intermolecular hydrogen bonds is identified at the core of the supramolecular column comprised of the first-generation hybrid dendrimer **3c** (Figure 2d). On the other hand, both intramolecular and intermolecular hydrogen bonds are possible between the twin dendrons. Such a network can be accommodated at the core of the resulting supramolecular column (Figure 2 h).

The existence of both Φ_h and *Pm* $\bar{3}$ *n* mesophases in the phase sequence of a single liquid crystalline dendron or dendrimer remains a rare phenomenon.^[10b,15d-g,16,20] Such behav-

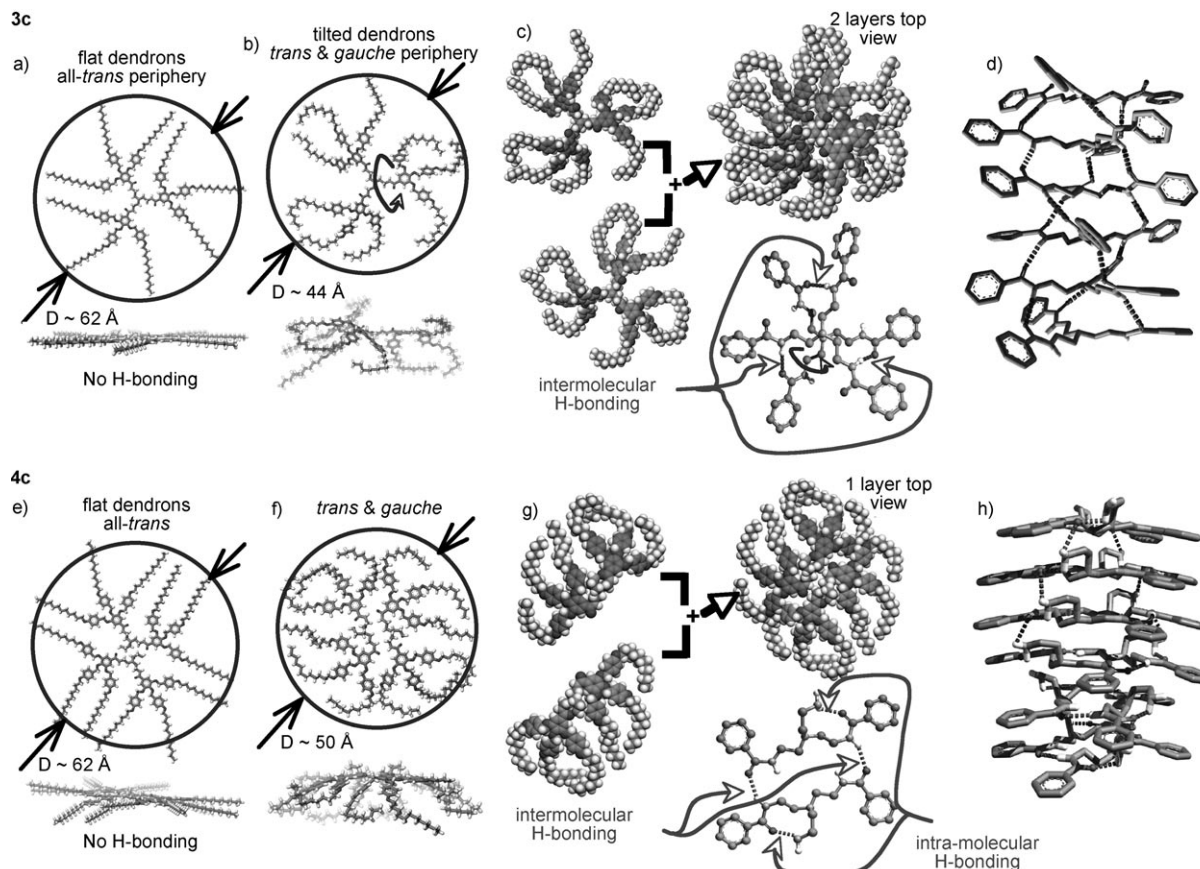


Figure 2. Molecular models of a)–d) **3c** and e)–h) **4c** shown in the all-*trans* flat dendrimer conformation (a and e), from the top and side stick views of the column strata (b and f), with the hydrogen-bonding network highlighted (c and g), and as a stick side view of the column core region (d and h).

ior can be valuable in elucidating the pathway by which the two phases are related.^[21] Epitaxial relationships between 2D hexagonal and 3D cubic mesophases in lyotropic liquid crystals^[21a,b] and block copolymers^[21c,d] suggest that cylindrical objects in the 2D hexagonal lattice form undulating columns, which subsequently form spherical objects through break points along the cylinder axis. Monodomains of the Φ_h lattice generated by **3c** have been prepared by extrusion of oriented fibers. These samples are amenable to XRD.

XRD patterns from oriented fiber samples of **3c** at various temperatures are presented in Figure 3a. The phase sequence described in Table 1 can be observed in the XRD patterns. Both the glass ($\Phi_{h,g}$) and the Φ_h mesophase show evidence of being well oriented with the q_{10} , q_{11} , and q_{20} reflections perpendicular to the fiber axis. Heating of the sample to generate the $Pm\bar{3}n$ mesophase transforms the diffraction pattern and indicates coincidence of the Φ_h q_{10} reflection and the $Pm\bar{3}n$ q_{211} reflection. This is indicative of a possible epitaxial relationship.^[21a] Figure 3b presents a schematic representation of the epitaxial relationship between the columns of the Φ_h lattice and the (111) direction of the $Pm\bar{3}n$ lattice. The six-fold axis of symmetry of the Φ_h lattice becomes the three-fold axis of symmetry of the $Pm\bar{3}n$ lattice. In keeping with previous explanations for such a relationship, we illustrate the transformation of the supramolecular cylinders into supramolecular spheres as proceeding through undulating columns. Recently a similar mechanism for columnar-to-cubic phase transitions was proposed for metallomesogens^[16] and “Janus-like” diblock codendrimers,^[20] although oriented fiber diffraction experiments were not reported.

Given the fast dynamics of the phase transition, it is not surprising that the preferred orientation of the Φ_h meso-

phase is not recovered upon cooling from the $Pm\bar{3}n$ mesophase.^[21c] Upon cooling oriented fiber samples from the $Pm\bar{3}n$ mesophase to the Φ_h mesophase, we observed no orientational order in the sample (Figure 3a). As the phase transition is reversible, the pathway by which spheres become cylinders should be the reverse of that by which cylinders become spheres (Figure 3b). Nonetheless, the 3D cubic lattice does not retain memory of the orientational order of the 2D columnar lattice. Consequently, domains of cylinders formed during cooling do not have a preferred orientation.

The models in Figure 2 allude to a possible molecular mechanism for pinch-point formation in the undulating columns in the proposed phase transformation. Necessarily, the columns shrink between two column strata. Transformation from the flat-taper conformation to the conical conformation can be rationalized as small reorientations of the TREN moiety. During this process, the self-assembling dendron fragments are forced into closer proximity. The net effect is similar to that observed for self-assembling dendrons comprised of 3,4- or 3,4,5-branching units; conical-shaped supramolecular building blocks emerge.^[6a,e,f,10b] The conical dendrons involve more extended molecular conformations (that is, with smaller α' values) than the flat-taper dendrons.^[22] Thus, at the peak of the undulation, which corresponds to the diameter of the newly forming spheres, the undulating column gets larger than the original column. Moving away from this location toward the pinch point, the conical molecules tilt away from their orientation in the column and this results in a constriction of the undulating column diameter below that of the original column. Eventually, the spheres separate into individual micellar aggregates.

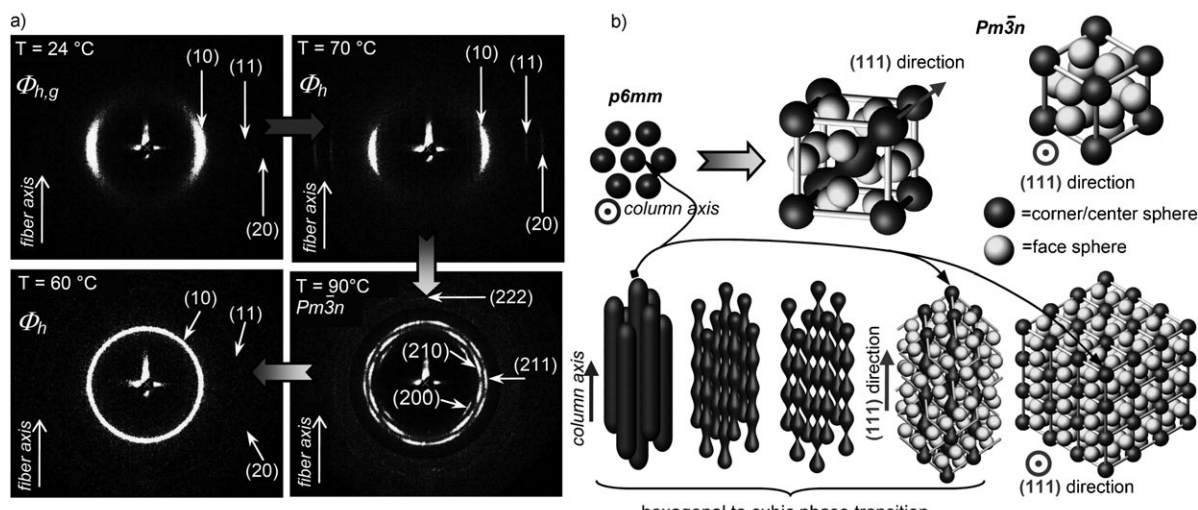


Figure 3. Epitaxial transition from the hexagonal to cubic phase observed for the **3c**. a) Small-angle XRD fiber patterns collected in the thermal cycle indicated by arrows; the lattice, temperatures, fiber orientation, and diffraction-peak indexing are marked. b) Schematic representation of the epitaxial relationship between the column axis in the hexagonal phase and the (111) direction of the cubic phase; the six-fold axis of symmetry of the columns becomes the three-fold axis of symmetry of the cubic phase. It is most likely that the weaker interactions present between the supramolecular spheres and the rearrangement of the face spheres (light gray) upon the transition from the oriented cubic to the hexagonal phase prohibit any epitaxial relationship. A set of corner/center spheres from the shown cubic lattice in (b) are colored in dark gray to show the connectivity.

Conclusion

First-generation hybrid dendrimers and their twin-dendron congeners comprised of self-assembling dendrons facilitate structural diversity at low generations. The dendrimers and twin dendrons have been prepared by coupling dendritic imidazolides and TREN. Structural and retrostructural analysis demonstrated that smectic, 2D Φ_{rc} , and Φ_h , as well as 3D cubic, lattices are formed. Just as for supramolecular dendrimers prepared from self-assembling dendrons, the primary structure of the constituent dendron manifests in the tertiary structure of the supramolecular object and the self-organized lattice. Quasiequivalence^[7a,c] of the self-assembling dendrons is further exploited by the flexibility of the dendrimer core, as we observe two new examples of thermoreversible shape change accompanied by optical property changes. Such behavior is demonstrative of rudimentary signaling or binary logic functions. Furthermore, the phase sequences reported herein have revealed an epitaxial relationship between the Φ_h and $Pm\bar{3}n$ lattices. We have postulated a mechanism by which a transition between the two mesophases can occur. Appending nonmesogenic dendrimers with self-assembling dendrons provides supramolecular structural diversity previously unavailable from low-generation dendrimers^[4,8] functionalized at their periphery with mesogens and heralds further opportunities when this approach is extended to higher generation self-assembling dendrons and other nonmesogenic dendrimer cores.

Experimental Section

Materials: 1,1'-Carbonyldiimidazole (CDI; Acros, 97%) was used as received. Its purity was assessed by melting-point measurement and ^1H NMR spectroscopy. Tris(2-aminoethyl)amine (TREN; Acros, 96%) was used as received. THF was refluxed over sodium ketyl until the solution turned purple and was then distilled before use. CH_2Cl_2 was freshly distilled from CaH_2 . Synthesis of imidazolides **2a–c** has been reported previously.^[13]

Techniques: All ^1H (500 MHz) and ^{13}C NMR (125 MHz) spectra were recorded on a Bruker DRX-500 instrument at 20°C with CDCl_3 as the solvent (tetramethylsilane (TMS) as an internal standard). DSC was performed on a Differential Scanning Calorimeter 2920 instrument (TA Instruments) at a rate of 5 °C min⁻¹. A polarized optical microscope (Olympus BX-60) equipped with a Mettler FP 82 hot stage was used to investigate the bulk properties of the compounds synthesized. All MALDI-TOF spectra were recorded on a Voyager-DE apparatus (Perceptive Bio-systems) with dihydroxybenzoic acid (Aldrich, 97%; recrystallized from water before use) as a matrix. The purity of the products was determined by a combination of techniques, including TLC on silica-gel plates (Kodak) with fluorescent indicator, HPLC with a Perkin-Elmer Series 10 high-pressure liquid chromatograph equipped with an LC-100 column oven, Nelson Analytical 900 Series integrator data station, and two Perkin-Elmer PL gel columns. Melting points were measured by using a Unimelt capillary melting point apparatus (Arthur H. Thomas Company, Philadelphia, USA). XRD measurements were performed by using $\text{Cu}_{\text{K}\alpha}$ radiation ($\lambda=1.54178 \text{ \AA}$) from a Bruker-Nonius FR-591 rotating anode X-ray source equipped with a $0.2 \times 0.2 \text{ mm}^2$ filament operated at 3.4 kW. The Cu radiation beam was collimated and focused by a single bent mirror and sagittally focused through an Si(111) monochromator, thereby generating a $0.3 \times 0.4 \text{ mm}^2$ spot on a Bruker-AXS Hi-Star multiwire area detector. To minimize attenuation and background scattering, an integral

vacuum was maintained along the length of the flight tube and within the sample chamber. Samples were held in quartz capillaries (0.7–1.0 mm in diameter), mounted in a temperature-controlled oven (temperature precision: $\pm 0.1^\circ\text{C}$; temperature range from -120 to 270°C). The distance between the sample and the detector was 12.0 cm for wide-angle diffraction experiments and 54.0 cm for intermediate-angle diffraction experiments. Aligned samples for fiber XRD experiments were prepared by using a custom-made extrusion device. Thus, powdered sample ($\approx 10 \text{ mg}$) was heated inside the extrusion device above the melt temperature. The fiber was extruded in the mesophase and cooled to 23°C . Typically, the aligned samples had a thickness of ≈ 0.3 – 0.7 mm and a length of ≈ 3 – 7 mm . All XRD measurements were done with the aligned-sample axis perpendicular to the beam direction. XRD peak position and intensity analysis was performed by using the Datasqueeze software (Version 2.01), which allows background elimination and Gaussian, Lorentzian, Lorentzian squared, or Voigt peak-shape fitting.

Typical procedure for coupling of imidazolides with TREN: Tris[2-(4-dodecan-1-yloxy)benzamido]ethylamine (3a): Imidazolide **2a** (0.712 g, 2.0 mmol) was dissolved in anhydrous THF. TREN (0.097 mL, 0.60 mmol) was added to the mixture through a syringe. The reaction mixture was stirred for 2 h at 22°C under an argon atmosphere. After completion of the reaction, the mixture was poured into water and the white precipitate was filtered off. Several recrystallizations from ethyl acetate afforded pure **3a** (0.539 g, 80%) as a white colorless powder: ^1H NMR (CDCl_3 , TMS): $\delta=0.87$ (t, 9H), 1.26 (m, 48H), 1.42 (m, 6H), 1.75 (m, 6H), 2.69 (t, 6H), 3.52 (t, 6H), 3.81 (t, 6H), 6.51 (d, 6H), 7.13 (t, 3H), 7.58 ppm (d, 6H); ^{13}C NMR (CDCl_3 , TMS): $\delta=14.51$, 23.10, 26.52, 29.72, 29.78, 29.95, 30.08, 30.13, 32.34, 38.10, 53.92, 68.45, 114.20, 126.28, 129.34, 161.89, 168.14 ppm; MALDI-TOF MS: m/z : 1049.29 [$M+\text{K}^+$], 1033.30 [$M+\text{Na}^+$], 1011.87 [M^+].

Tris(2-[3,4-bis[(4'-dodecan-1-yloxy)benzyloxy]benzamido]ethyl)amine (3b):

A procedure analogous to that described above was employed. After several recrystallizations from acetone, **3b** (94% yield) was obtained as a colorless solid: ^1H NMR (CDCl_3 , TMS): $\delta=0.88$ (t, 18H), 1.26 (m, 96H), 1.43 (m, 12H), 1.74 (m, 12H), 2.72 (m, 6H), 3.56 (m, 6H), 3.87–3.81 (overlapped m, 12H), 4.69 (s, 6H), 4.87 (s, 6H), 6.28 (d, 3H), 6.65 (dd, 12H), 7.02 (d, 12H), 7.16 (d, 6H), 7.53 ppm (d, 3H); ^{13}C NMR (CDCl_3 , TMS): $\delta=14.51$, 23.10, 26.52, 26.58, 29.78, 29.87, 29.99, 30.05, 30.09, 30.11, 30.14, 32.35, 38.15, 53.86, 68.38, 70.90, 71.67, 113.08, 114.54, 114.68, 115.21, 120.95, 126.89, 128.72, 129.20, 129.70, 148.84, 152.40, 159.25, 168.13 ppm; MALDI-TOF MS: m/z : 2237.33 [$M+\text{K}^+$], 2221.18 [$M+\text{Na}^+$], 2199.87 [M^+].

Tris(2-[3,4,5-tris[(4'-dodecan-1-yloxy)benzyloxy]benzamido]ethyl)amine (3c):

A procedure analogous to that described above was employed. The product was purified by column chromatography on silica, with first a CH_2Cl_2 /ethyl acetate mixture and then a chloroform/methanol mixture as the eluting solvent, with subsequent evaporation of the solvent. Pure product was isolated as waxy colorless solid in 79% yield: ^1H NMR (CDCl_3 , TMS): $\delta=0.88$ (t, 27H), 1.26 (m, 144H), 1.41 (m, 18H), 1.74 (m, 18H), 2.72 (m, 6H), 3.52 (m, 6H), 3.87–3.81 (overlapped m, 18H), 4.76 (s, 12H), 4.78 (s, 6H), 6.65 (d, 6H), 6.73 (d, 12H), 7.17–7.09 (overlapped m, 24H), 7.25 ppm (m, 3H); ^{13}C NMR (CDCl_3 , TMS): $\delta=14.51$, 23.10, 26.58, 26.53, 29.79, 29.95, 30.09, 30.13, 32.34, 39.75, 56.82, 68.37, 71.37, 75.09, 107.23, 114.40, 114.67, 129.05, 129.53, 129.73, 130.17, 130.41, 141.80, 153.22, 159.21, 168.18 ppm; MALDI-TOF MS: m/z : 3107.97 [$M+\text{K}^+$], 3092.04 [$M+\text{Na}^+$], 3071.48 [M^+].

2-[N,N-Bis(2-[3,4-bis[(4'-dodecan-1-yloxy)benzyl]benzamido]ethyl)amino]ethylamine (4b):

This compound was isolated by column chromatography as a byproduct from the incomplete acylation of TREN by **2b**. When the chromatographic separation and purification method described above was applied to the mixture of products, **4b** was isolated as a yellowish solid: ^1H NMR (CDCl_3 , TMS): $\delta=0.87$ (t, 12H), 1.26 (m, 64H), 1.41 (m, 8H), 1.76 (m, 10H), 2.57 (t, 2H), 2.72 (t, 4H), 2.74 (t, 2H), 3.50 (q, 4H), 3.90 (t, 8H), 4.90 (s, 4H), 4.96 (s, 4H), 6.37 (d, 2H), 6.82 (overlapped m, 8H), 7.24 (dd, 10H), 7.32 (t, 2H), 7.51 ppm (d, 2H); ^{13}C NMR (CDCl_3 , TMS): $\delta=14.52$, 23.10, 26.50, 29.77, 29.88, 30.06, 30.10, 32.34, 38.52, 40.02, 68.43, 71.16, 71.47, 113.84, 114.73, 114.79, 120.63, 127.71, 128.89, 129.22, 129.44, 129.59, 149.07, 152.14, 159.33, 167.72 ppm;

MALDI-TOF MS: m/z : 1054.79 [$M+K^+$], 1539.30 [$M+Na^+$], 1516.87 [M^+].

2-[*N,N*-Bis(2-(3,4,5-tris(4'-dodecan-1-yloxy)benzoyloxy)benzamido]ethyl]-amino]ethylamine (4c**):** This compound was isolated by column chromatography as a byproduct from the incomplete acylation of TREN by **2c**. When the chromatography separation and purification method described above was applied to the mixture of products, **4c** was isolated as a yellowish solid: ^1H NMR (CDCl_3 , TMS): δ = 0.87 (t, 18H), 1.26 (m, 96H), 1.43 (m, 16H), 1.76 (m, 18H), 2.59 (m, 2H), 2.71 (m, 6H), 3.52 (m, 4H), 3.89 (m, 12H), 4.84 (s, 4H), 4.85 (s, 8H), 6.66 (d, 4H), 6.80 (d, 8H), 7.25–7.13 ppm (m, 18H); ^{13}C NMR (CDCl_3 , TMS): δ = 14.50, 23.09, 26.52, 29.77, 29.90, 30.06, 30.10, 32.33, 39.09, 40.13, 54.39, 56.37, 68.38, 68.47, 71.41, 107.39, 114.43, 114.76, 114.79, 129.24, 129.62, 129.94, 130.18, 130.46, 141.69, 153.13, 159.33, 168.08 ppm; MALDI-TOF MS: m/z : 2135.10 [$M+K^+$], 2118.53 [$M+Na^+$], 2096.33 [M^+].

Acknowledgements

Financial support by the National Science Foundation (grant nos.: DMR-05-48559 and DMR-05-20020), DuPont-Marshall Laboratories, and the P. Roy Vagelos Chair at the University of Pennsylvania is gratefully acknowledged.

- [1] a) E. Buhleier, W. Wehner, F. Vögtle, *Synthesis* **1978**, 155–158; b) D. A. Tomalia, H. Baker, J. Dewald, M. Hall, G. Kallos, S. Martin, J. Roeck, J. Ryder, P. Smith, *Polym. J.* **1985**, 17, 117–132; c) G. R. Newkome, Z. Yao, G. R. Baker, V. K. Gupta, *J. Org. Chem.* **1985**, 50, 2003–2004.
- [2] a) C. J. Hawker, J. M. J. Fréchet, *J. Am. Chem. Soc.* **1990**, 112, 7638–7647; b) T. M. Miller, T. X. Neenan, *Chem. Mater.* **1990**, 2, 346–349.
- [3] a) J. M. J. Fréchet, D. A. Tomalia in *Dendrimers and Other Dendritic Polymers*, Wiley, New York, **2001**; b) G. R. Newkome, C. N. Moorefield, F. Vögtle, *Dendrimers and Dendrons*, Wiley-VCH, Weinheim, **2001**; c) V. Percec, *Phil. Trans. R. Soc. A* **2006**, 364, 2709–2719.
- [4] a) S. A. Ponomarenko, N. I. Boiko, V. P. Shibaev, *Polym. Sci. Ser. C* **2001**, 43, 1601–1650; b) B. Donnio, D. Guillou, *Adv. Polym. Sci.* **2006**, 201, 45–155.
- [5] a) V. Percec, P. Chu, G. Ungar, J. Zhou, *J. Am. Chem. Soc.* **1995**, 117, 11441–11454; b) V. Percec, P. Chu, M. Kawasumi, *Macromolecules* **1994**, 27, 4441–4453; c) V. Percec, M. Kawasumi, *Macromolecules* **1992**, 25, 3843–3850; d) V. Percec, C. G. Cho, C. Pugh, D. Tomazos, *Macromolecules* **1992**, 25, 1164–1176.
- [6] a) S. D. Hudson, H.-T. Jung, V. Percec, W.-D. Cho, G. Johansson, G. Ungar, V. S. K. Balagurusamy, *Science* **1997**, 278, 449–452; b) G. Ungar, Y. Liu, X. Zeng, V. Percec, W.-D. Cho, *Science* **2003**, 299, 1208–1211; c) X. Zeng, G. Ungar, Y. Liu, V. Percec, A. E. Dulcey, J. K. Hobbs, *Nature* **2004**, 428, 157–160; d) V. Percec, A. E. Dulcey, V. S. K. Balagurusamy, Y. Miura, J. Smidrkal, M. Peterca, S. Nummelin, U. Edlund, S. D. Hudson, P. A. Heiney, H. Duan, S. N. Magonov, S. A. Vinogradov, *Nature* **2004**, 430, 764–768; e) V. S. K. Balagurusamy, G. Ungar, V. Percec, G. Johansson, *J. Am. Chem. Soc.* **1997**, 119, 1539–1555; f) D. R. Dukeson, G. Ungar, V. S. K. Balagurusamy, V. Percec, G. A. Johansson, M. Glodde, *J. Am. Chem. Soc.* **2003**, 125, 15974–15980; g) V. Percec, W.-D. Cho, M. Möller, S. A. Prokhorova, G. Ungar, D. J. P. Yeardley, *J. Am. Chem. Soc.* **2000**, 122, 4249–4250.
- [7] a) V. Percec, C.-H. Anh, G. Ungar, D. J. P. Yeardley, M. Möller, S. S. Sheiko, *Nature* **1998**, 391, 161–164; b) V. Percec, M. Glodde, T. K. Bera, Y. Miura, I. Shiyankovskaya, K. D. Singer, H.-W. Spiess, S. D. Hudson, H. Duan, *Nature* **2002**, 419, 384–387; c) V. Percec, M. N. Holerca, *Biomacromolecules* **2000**, 1, 6–16; d) Y. K. Kwon, S. Chvalun, A.-I. Schneider, J. Blackwell, V. Percec, J. A. Heck, *Macromolecules* **1994**, 27, 6129–6132; e) V. Percec, J. A. Heck, D. Tomazos, G. Ungar, *J. Chem. Soc. Perkin Trans. 2* **1993**, 2381–2388; f) V. Percec, D. Schlueter, *Macromolecules* **1997**, 30, 5783–5790; g) V. Percec, D. Schlueter, J. C. Ronda, G. Johansson, G. Ungar, J. P. Zhou, *Macromolecules* **1996**, 29, 1464–1472; h) V. Percec, D. Schlueter, G. Ungar, S. Z. D. Cheng, A. Zhang, *Macromolecules* **1998**, 31, 1745–1762; i) Y. K. Kwon, S. N. Chvalun, J. Blackwell, V. Percec, J. A. Heck, *Macromolecules* **1995**, 28, 1552–1558.
- [8] a) S. A. Ponomarenko, E. A. Rebrov, N. I. Boiko, N. G. Vasilenko, A. M. Muzaferov, Y. S. Freidzon, V. P. Shibaev, *Polym. Sci. Ser. A* **1994**, 36, 896–901; b) U. Stebani, G. Lattermann, *Adv. Mater.* **1995**, 7, 578–581; c) U. Stebani, G. Lattermann, M. Wittenberg, J. H. Wendorff, *Angew. Chem.* **1996**, 108, 1941–1943; *Angew. Chem. Int. Ed. Engl.* **1996**, 35, 1858–1861; d) M. C. Coen, K. Lorenz, J. Kressler, H. Frey, R. Mühlaupt, *Macromolecules* **1996**, 29, 8069–8076; e) M. W. P. L. Baars, S. H. M. Söntjens, H. M. Fischer, H. W. L. Peirlings, E. W. Meijer, *Chem. Eur. J.* **1998**, 4, 2456–2466; f) J. Barberá, M. Marcos, J. L. Serrano, *Chem. Eur. J.* **1999**, 5, 1834–1840; g) M. Katoh, S. Uehara, S. Kohimoto, K. Kishikawa, *Chem. Lett.* **2006**, 35, 322–323.
- [9] V. Percec, B. C. Won, M. Peterca, P. A. Heiney, *J. Am. Chem. Soc.* **2007**, 129, 11265–11278.
- [10] a) V. Percec, W.-D. Cho, G. Ungar, D. J. P. Yeardley, *Angew. Chem.* **2000**, 112, 1661–1666; *Angew. Chem. Int. Ed.* **2000**, 39, 1597–1602; b) V. Percec, W.-D. Cho, G. Ungar, *J. Am. Chem. Soc.* **2000**, 122, 10273–10281.
- [11] a) V. Percec, C. M. Mitchell, W.-D. Cho, S. Uchida, M. Glodde, G. Ungar, X. Zeng, Y. Liu, V. S. K. Balagurusamy, P. A. Heiney, *J. Am. Chem. Soc.* **2004**, 126, 6078–6094; b) V. Percec, M. N. Holerca, S. Nummelin, J. J. Morrison, M. Glodde, J. Smidrkal, M. Peterca, B. M. Rosen, S. Uchida, V. S. K. Balagurusamy, M. J. Sienkowska, P. A. Heiney, *Chem. Eur. J.* **2006**, 12, 6216–6241; c) V. Percec, J. Smidrkal, M. Peterca, C. M. Mitchell, S. Nummelin, A. E. Dulcey, M. J. Sienkowska, P. A. Heiney, *Chem. Eur. J.* **2007**, 13, 3989–4007.
- [12] a) A. Pegenau, T. Hegmann, C. Tschiesske, S. Diele, *Chem. Eur. J.* **1999**, 5, 1643–1660; b) A. Pegenau, X. H. Cheng, C. Tschiesske, P. Göring, S. Diele, *New J. Chem.* **1999**, 23, 465–467; c) T. Hatano, T. Kato, *Chem. Commun.* **2006**, 1277–1279.
- [13] V. Percec, M. Peterca, M. E. Yurchenko, J. G. Rudick, P. A. Heiney, *Chem. Eur. J.* **2007**, 14, 909–918.
- [14] a) V. Percec, C.-H. Anh, T. K. Bera, G. Ungar, D. J. P. Yeardley, *Chem. Eur. J.* **1999**, 5, 1070–1083; b) V. Percec, T. K. Bera, M. Glodde, Q. Fu, V. S. K. Balagurusamy, P. A. Heiney, *Chem. Eur. J.* **2003**, 9, 921–935; c) V. Percec, M. R. Imam, T. K. Bera, V. S. K. Balagurusamy, M. Peterca, P. A. Heiney, *Angew. Chem.* **2005**, 117, 4817–4823; *Angew. Chem. Int. Ed.* **2005**, 44, 4739–4745.
- [15] a) U. Stebani, G. Lattermann, M. Wittenberg, R. Festag, J. H. Wendorff, *Adv. Mater.* **1994**, 6, 572–577; b) U. Stebani, G. Lattermann, *Macromol. Rep.* **1995**, A32, 385–401; c) H. Fischer, S. S. Ghosh, P. A. Heiney, N. C. Maliszewskyj, T. Plesnivý, H. Ringsdorf, M. Seitz, *Angew. Chem.* **1995**, 107, 1941–1957; *Angew. Chem. Int. Ed. Engl.* **1995**, 34, 1795–1798; d) D. J. P. Yeardley, G. Ungar, V. Percec, M. N. Holerca, G. Johansson, *J. Am. Chem. Soc.* **2000**, 122, 1684–1689; e) H. Duan, S. D. Hudson, G. Ungar, M. N. Holerca, V. Percec, *Chem. Eur. J.* **2001**, 7, 4134–4141; f) V. Percec, M. N. Holerca, S. N. Magonov, D. J. P. Yeardley, G. Ungar, H. Duan, S. D. Hudson, *Biomacromolecules* **2001**, 2, 706–728; g) V. Percec, M. N. Holerca, S. Uchida, D. J. P. Yeardley, G. Ungar, *Biomacromolecules* **2001**, 2, 729–740.
- [16] B. Donnio, B. Heinrich, T. Gulik-Krzywicki, H. Delacroix, D. Guillot, D. W. Bruce, *Chem. Mater.* **1997**, 9, 2951–2965.
- [17] a) G. Lattermann, *Liq. Cryst.* **1989**, 6, 619–625; b) S. H. J. Idziak, N. C. Maliszewskyj, G. B. M. Vaughan, P. A. Heiney, C. Mertesdorf, H. Ringsdorf, J. P. McCauley Jr., A. B. Smith III, *J. Chem. Soc. Chem. Commun.* **1992**, 98–99; c) J.-M. Lehn, J. Malthête, A.-M. Levelut, *J. Chem. Soc. Chem. Commun.* **1985**, 1794–1796.
- [18] a) H. A. Staab, *Angew. Chem.* **1962**, 74, 407–423; *Angew. Chem. Int. Ed. Engl.* **1962**, 1, 351–367; b) S. P. Rannard, N. J. Davis, *Org. Lett.* **1999**, 1, 933–936; c) S. P. Rannard, N. J. Davis, *Org. Lett.* **2000**, 2, 2117–2120; d) S. Rannard, N. Davis, H. McFarland, *Polym. Int.* **2000**, 49, 1002–1006.

- [19] S. N. Chvalun, M. A. Shcherbina, A. N. Yakunin, J. Blackwell, V. Percec, *Polym. Sci. Ser. A* **2007**, *49*, 158–167.
- [20] I. Bury, B. Heinrich, C. Bourgogne, D. Guillou, B. Donnio, *Chem. Eur. J.* **2006**, *12*, 8396–8413.
- [21] a) P. Mariani, L. Q. Amaral, L. Saturni, H. Delacroix, *J. Phys. II* **1994**, *4*, 1393–1416; b) P. Sakaya, J. M. Seddon, R. H. Templer, R. J. Mirkin, G. J. T. Tiddy, *Langmuir* **1997**, *13*, 3706–3714; c) M. F. Schulz, F. S. Bates, K. Almdal, K. Mortensen, *Phys. Rev. Lett.* **1994**, *73*, 86–89; d) M. W. Matsen, *J. Chem. Phys.* **2001**, *114*, 8165–8173.
- [22] G. Ungar, V. Percec, M. N. Holerca, G. Johansson, J. A. Heck, *Chem. Eur. J.* **2000**, *6*, 1258–1266.

Received: October 21, 2007

Revised: December 15, 2007

Published online: February 12, 2008